

Article

Pyrolysis of Rapeseed Oil Press Cake and Steam Gasification of Solid Residues

Lech Nowicki ¹, Dorota Siuta ^{1,*}  and Maciej Markowski ²

¹ Faculty of Process and Environmental Engineering, Lodz University of Technology, Wolczanska 213, 90-924 Lodz, Poland; lech.nowicki@p.lodz.pl

² EKO-SERWIS S.C., Wierzbowa 48, 90-133 Lodz, Poland; markowski.m.p@gmail.com

* Correspondence: dorota.siuta@p.lodz.pl; Tel.: +48-426313743

Received: 23 July 2020; Accepted: 25 August 2020; Published: 31 August 2020



Abstract: A deoiled rapeseed press cake (RPC) was pyrolyzed by heating at a slow heating rate to 1000 °C in a fixed bed reactor, and the produced char was then gasified to obtain data for the kinetic modeling of the process. The gasification experiments were performed in a thermogravimetric analyzer (TGA) under steam/argon mixtures at different temperatures (750, 800 and 850 °C) and steam mole fractions (0.17 and 0.45). The three most commonly used gas-solid kinetic models, the random pore model, the volumetric model and the shrinking core model were used to describe the conversion of char during steam gasification. The objective of the kinetic study was to determine the kinetic parameters and to assess the ability of the models to predict the RPC conversion during steam gasification. A TGA-MS analysis was applied to assess the composition of the product gas. The main steam gasification product of the RPC was hydrogen (approximately 60 mol % of the total product). The volumetric model was able to accurately predict the behavior of the RPC char gasification with steam at temperatures of 750–850 °C and steam concentrations less than 0.45 mole fraction. The activation energy and the reaction order with respect to steam were equal to 166 kJ/mol and 0.5, respectively, and were typical values for the gasification of biomass chars with steam

Keywords: steam gasification; kinetics; rapeseed oil press cake; synthesis gas; TGA-MS analysis; pyrolysis

1. Introduction

Biofuels derived from the chemical processing of plant biomass, have emerged as one of the most viable alternatives to petroleum fuels. In Europe, rapeseed oil is the most popular and inexpensive material to produce biofuels. Biodiesel from vegetable oil is a natural fuel composed mainly of methyl esters of long-chain fatty acids obtained by the transesterification reaction of triglycerides contained in the oil with alcohols in the presence of a hydroxide catalyst (KOH, NaOH, etc.) [1,2]. Typically, in biodiesel production processes, anhydrous methanol is used, mainly due to its cost and its physical and chemical advantages [3]. For the basic-catalyzed process of transesterification, a significant amount of alcohol is used. The optimal molar ratio of methanol to oil is 6/1 [1].

Under industrial conditions, rapeseed oil is usually received by cold pressing rapeseeds on mechanical presses. After pressing a rapeseed press cake (RPC) is produced (450–550 kg from 1 Mg of seeds [4]) as a solid byproduct. RPC is a carbon, oxygen rich biomass containing a low amount of hydrogen and trace amounts of nitrogen and sulfur. It is composed mainly of lignin, hemicellulose, cellulose and lower amounts of other organic compounds [5–8].

As it is widely acknowledged in literature that the most promising and convenient technologies to convert RPC into valuable products are pyrolysis and gasification [9,10]. Pyrolysis is a process of the thermal decomposition of material in the absence of oxygen to produce three types of products: a liquid fraction, uncondensable gases and solid residue—char. By choosing specific pyrolysis conditions, it is

possible to maximize the production of one particular fraction. In this case, the key parameters are the heating rate, final pyrolysis temperature and vapor residence time in the reactor. Based on the heating rate and pyrolysis time, three types of pyrolysis are differentiated as follows: slow, fast and flash. Fast and flash pyrolysis, which have reaction times less than 2 s, produces large amounts of liquid product, while slow pyrolysis is employed to maximize the solid product yield [11,12].

The first RPC slow pyrolysis studies were conducted in Turkey using a laboratory scale fixed bed reactor [5,11,13]. The distribution and characteristics of products were investigated at different final pyrolysis temperatures. For example, at temperature of 500 °C was as follows (in wt % of the initial mass converted): liquid fraction 59.7 %, gas fraction 12.7 % and solid residue 27.4 % [5]. Similar tests but in a wider temperature range were performed by Ucar and Ozkan [6]. Their results showed that water and bio-char were the main pyrolysis products irrespective of temperature. The yield of the latter product decreased from 38.4 to 30.0 wt % with increasing the temperature from 400 to 900 °C. The yield of organic phase of liquid product was initially increased with increasing the temperature, reached its maximum value of 18.6 wt % at 500 °C and then dropped slightly. At this temperature only about 8 % of the sample mass was converted into gas fraction of the products. The pyrolysis gas was composed of CO₂, CO, C₁–C₇ hydrocarbons and H₂S. Organic product (bio-oil) contained a large group of substances including fatty acids, aromatic and heterocyclic organic compounds. The effect of particle size, pyrolysis temperature, carrier gas flow rate in a fixed bed reactor for pyrolysis of RPC was investigated by David and Kopac [14]. Optimum parameters obtained for the maximum liquid quantity and bio-oil yield (49.8 and 38.7 %, respectively) were particle size range less than 0.5 mm and the temperature 500 °C. At these conditions, the yield of gas and solid products was 39.2 and 12.1 %, respectively. As can be seen, these results are not consistent with those obtained by Ucar and Ozkan [6]. The reason for the discrepancies was probably due to different gas residence times during the heating up the sample in the reactor.

Possibilities of flash pyrolysis to convert RPC into a liquid form in a lab-scale reactor was studied by Smets et al. [7]. They found that at 550 °C the bio-oil fraction reached a maximum yield of 42.1 wt % of the initial sample mass [15], so it was much higher than for slow pyrolysis, as expected. The oil fraction analysis showed compounds related to triglycerides. Only 17 wt % of initial mass containing 71 % of carbon remained as a solid residue at the pyrolysis temperature of 550 °C and the yield of gas fraction was 24.1 wt. % at this temperature.

In the pyrolysis process a certain amount of char containing pure carbon is always produced and it has the potential to be utilized to improve the biomass conversion efficiency. Because the char produced during biomass pyrolysis is highly reactive it can be easily gasified with H₂O, oxygen, CO₂ or a combination of these gases to generate hydrogen or carbon monoxide to create syngas [16,17].

Biomass is usually gasified in a one-stage process where pyrolysis and char gasification occur in one reactor. The gasification product contains hydrogen, carbon oxide, carbon dioxide, methane, and a lower amount of many other compounds [18]. The gas produced in the one-step gasification of biomass was basically used for heat and electricity production. However, increasing attention has been devoted to applying it in organic synthesis [19]. In this case, the syngas has to meet specific quality requirements concerning the composition and purity. For example, an important parameter to consider is the molar ratio of hydrogen to carbon monoxide, which for most syntheses should be at least 2 [20–22]. Typically, the H₂/CO ratio of the syngas obtained from biomass gasification is between 1 and 2.2 [23]. This ratio can be adjusted in a separate catalytic reactor before the synthesis reactor, where part of the CO is transformed into hydrogen by the water-gas shift reaction [23,24].

Syngas produced in one step by conventional gasification usually contains impurities such as hydrogen sulfide, ammonia, hydrogen chloride and tars. To achieve better quality standards for the catalytic synthesis processes, syngas must undergo cleaning. An effective method to achieve the conversion of biomass to synthesis gas with low contaminants seems to be a two-stage process where the biomass is pyrolyzed in the first step and the char is subjected to a gasification process in a separate reactor [25]. By using a suitable gasification agent and temperature, the synthesis gas of

any composition can be obtained. Separation of the volatile fraction from char before gasification will significantly increase the purity of the synthesis gas. This mainly applies to sulfur, which is always present in the raw RPC [5–9], and can cause rapid deactivation of many CO hydrogenation catalysts [20,26]. Using pure steam as a gasification agent provides a synthesis gas with a high H₂/CO ratio [27] that is beneficial for synthetic natural gas (SNG), methanol or Fischer–Tropsch synthesis.

The CO₂ gasification of RPC char was only studied experimentally using thermogravimetric analysis by Nowicki et al. [15] but still there are no experimental data and kinetic parameters that describe the RPC char gasification with steam. Therefore, the present research is intended to provide information about steam gasification of rapeseed residues produced by high temperature slow pyrolysis and kinetic modeling.

2. Materials and Methods

2.1. Materials

The rapeseed oil press cake obtained from the Bio-Tech LTD plant, located in Lask (Poland), was used during the pyrolysis process for the production of char. The RPC samples were previously dried in an oven at 105 °C for 24 h to reduce their moisture and then crushed in a laboratory mill (Fritsch Pulverisette 15, Weimar, Germany).

The proximate and ultimate analyses of the RPC were performed using an elemental analyzer (CE Instruments NA 2500, Hindley Green, UK) and a thermogravimetric analyzer (Mettler-Toledo TGA/SDTA851 LF, Greifensee, Switzerland), and the results are listed in Table 1.

Table 1. Physical and chemical composition of the rapeseed press cake (RPC) and RPC char (wt %).

Sample	Moisture	Volatiles	Fixed Carbon	Ash	C	H	N	S
RPC	6.6	66.5	18.6	8.0	45.9	6.8	5.8	0.4
Char from RPC	-	-	74.0	26.0	57.3	0.6	4.5	0.1

2.2. Experiments

A horizontal fixed-bed reactor (with a 20 mm internal diameter and 0.9 m long) heated by an electric furnace was used to produce char by devolatilization of the RPC for the gasification tests. Dried samples were heated up to 1000 °C at a constant rate 10 °C/min in atmosphere of argon with flow rate at 100 cm³/min, after reaching final temperature samples were maintained for 60 min and cooled to ambient temperature and then sieved to the char particle size of 70–125 μm. The char characteristics after the RPC pyrolysis are combined in Table 1.

Gasification experiments of RPC chars were carried out in a STA 409 PG (Netzsch, Selb, Germany) thermobalance that was equipped with a water vapor furnace, which enabled measurements in a controlled atmosphere of steam and argon. The mass spectrometer (Balzers ThermoStar QMS 200, Asslar, Germany) was connected to the thermobalance to measure the product gas composition.

Preliminary gasification tests of chars derived from the RPC were conducted under dynamic conditions in which 50 mg samples were heated from room temperature to 1050 °C at a rate of 10 °C/min, and the data used for developing the rate equations were collected under isothermal conditions at 750, 800, and 850 °C. In both types of experiments, a mixture of steam (17 or 45 mol %) and argon was used that flowed over the sample at a rate of 50 cm³/min.

3. Results and Discussion

3.1. Products from the RPC Char during Steam Gasification

Variations in the sample mass and differential thermogravimetry (DTG) signals with temperature during steam gasification of the RPC obtained in two tests carried out under the same conditions are given in Figure 1. These experiments were performed to establish the temperatures at which

the reaction occurs at a reasonable rate. As shown in Figure 1, the reaction occurs completely at temperatures from 600 to 950 °C, and the maximum rate of the RPC steam gasification was observed at approximately 843 °C.

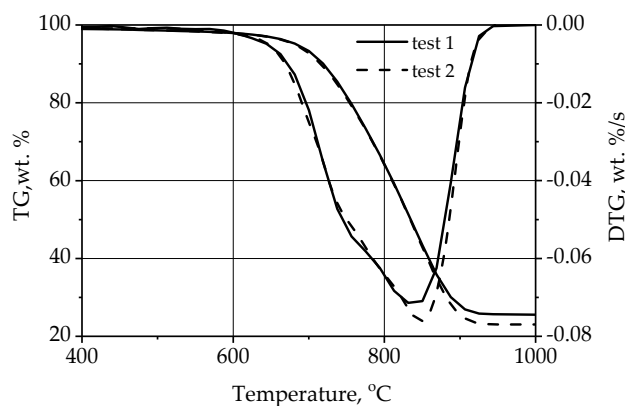


Figure 1. TGA and differential thermogravimetry (DTG) signals for the steam gasification of char derived from RPC. (heating rate 10 °C/min in 17 mol. % H₂O concentration under argon).

The evolution of the various gas products from the gasification of RPC char was also measured in tests using mass spectrometry (MS). The following ions, which are characteristic of the molecules of interest, were monitored: H₂ (m/z = 2), H₂O (m/z = 18), CO (m/z = 28), Ar (m/z = 40), CO₂ (m/z = 44), and CH₄ (m/z = 16). The DTG curves together with the primary ion intensities, which show the evolution profiles of the gasification products of the RPC char are presented in Figure 2.

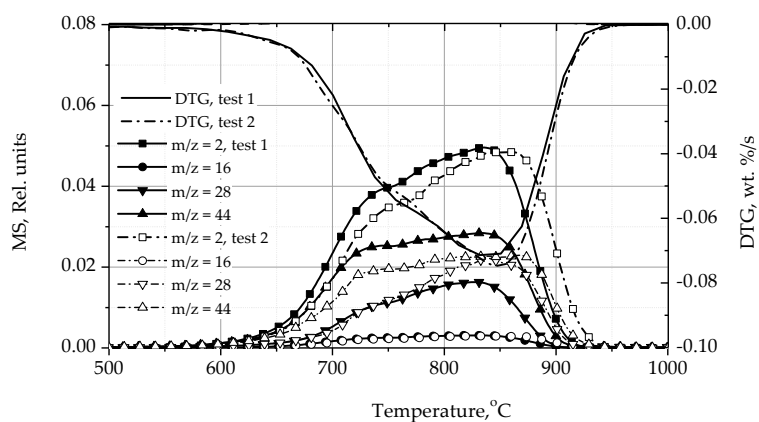


Figure 2. Mass spectrometry (MS) and DTG plots for the steam gasification products of the RPC char (17 mol % H₂O in Ar).

To obtain an approximate composition of gas from MS measurements, the procedure was applied described in [28,29]. The estimated composition of gases (Table 2) during gasification of the RPC char with steam was similar for different conditions (isothermal and non-isothermal) and methods of conducting experiments. Volatile products such as H₂, CH₄, CO, CO₂, were respectively equal to 61–63, 1–2, 7–12 and 25–29 mol %. As shown in Figures 1 and 2 the results obtained in the two tests are quite similar, indicating good reproducibility of the measured variables.

Table 2. The calculated composition of gases using the procedure presented in [28,29].

H ₂ O Conc., mol %	Temperature, °C	Gas Product Composition, mol %			
		H ₂	CH ₄	CO	CO ₂
17	600–950	62	1	8	29
		61	1	10	28
17	850	62	1	12	25
45	850	62	1	9	28
45	800	63	1	9	28
45	750	63	2	7	27

Steam gasification involves the primary reaction of water with atomic carbon contained in char to produce syngas, according to Equation (1):



A significant amount of carbon dioxide in the product gas indicates a high activity of the water-gas shift (WGS) reaction (Equation (2)), which converts CO into CO₂



A complex mechanism of steam gasification can be seen in the DTG and MS curves shown in Figure 2, which are composed of two dominant peaks. The first peak with a maximum at 747–756 °C is assigned to the reaction of carbon with H₂O (Equation (1)), whereas the second peak with a maximum at 843 °C represents the secondary reaction (Equation (2)), which needs higher temperatures to occur as depicted in our previous work [29]. We can suppose that the inorganic compounds contained in char provide active sites for the WGS reaction to proceed and that this material can also act as a catalyst for the methanation reaction that is responsible for the formation of methane present in the gas product.

On the basis of the product gas composition and the amount of carbon in the reacted char, the yield of the steam gasification was estimated to be equal to 3.68 Nm³ per kg of RPC char. The high hydrogen concentration, H₂/CO ratio of 6/1 and relatively high CO₂ content in the produced gas obtained in this work have also been previously reported by other authors [17,30].

3.2. Kinetics of RPC Char Gasification

RPC char gasification tests were performed under atmospheric pressure at three temperatures of 750, 800, and 850 °C and under isothermal conditions. As gasifying agents, mixtures of steam (17 and 45 mol %) diluted with argon were used. Once the desired temperature was attained, an adequate amount of water was introduced into the gas stream to ensure proper steam concentration. The TGA data were transferred to the conversion rate (*X*) by the following Equation (3):

$$X = \frac{m_0 - m}{m_0 - m_F} \quad (3)$$

where *m*₀, *m* and *m*_F are the initial, instantaneous and final RPC char weights during steam gasification, respectively.

Three gas-solid kinetic models such as the random pore model (RPM), the volumetric model (VM) and the shrinking core model (SCM) were applied to obtain kinetic parameters. Detailed descriptions, assumptions and equations of the tested reaction rate models of gasification reactions of char can be found in [15,31–33].

Comparisons between experimentally determined the RPC char conversions and results obtained from the volumetric model are illustrated in Figure 3 where symbols represent the raw data and the

lines present the best fitting model predictions. These results show the effects of the steam concentration (17 and 45 mol %) and temperature (750, 800, and 850 °C) on the reaction times.

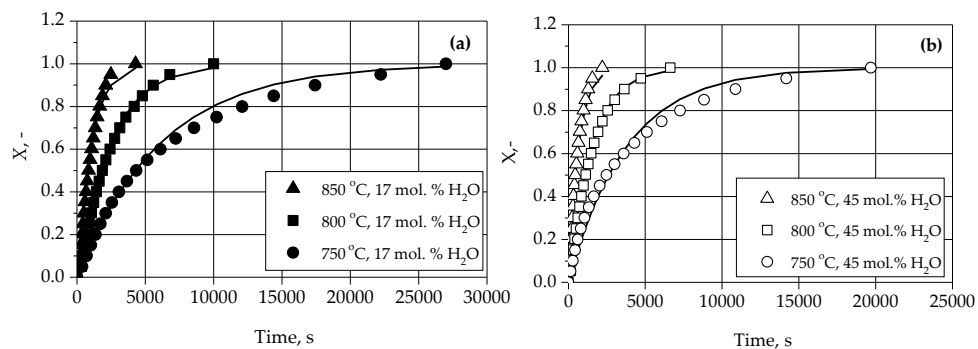


Figure 3. RPC char conversion versus reaction time for the VM (described by Equation (6)), which was the best fitting model prediction for (a) 17 mol % H₂O in Ar, (b) 45 mol % H₂O in Ar.

As shown in Figure 4, the RPC char reactivity (dX/dt) during steam gasification is not the same under different operating conditions. In the cases where reaction rates are higher, a maximum occurs on the reactivity profiles at 10–20 % conversion, while at lower reaction rates, such a maximum does not appear. Thus, it is difficult to clearly establish which of the kinetic models is the best in predicting the reaction rate in the tested temperature and steam concentration range. In such a situation, three tested kinetic models were evaluated based on the available experimental data in a range of conversion from 0.05 to 0.95.

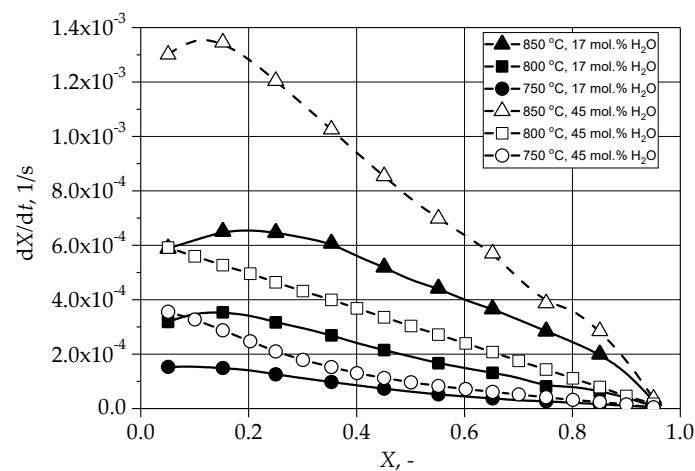


Figure 4. Reactivity of RPC char under different temperatures (750, 800 and 850 °C) and steam mole fractions (0.17 and 0.45) for the VM.

To evaluate the models, the approximate values of unknown three model parameters were determined; then, nonlinear regression using the minimization of squared residuals method was applied to obtain their final parameter values with three rate equations shown in our previous work [15]. Initially, the reaction rate constants (k_s) for the different steam mole fractions (0.17 and 0.45) and temperatures (750, 800 and 850 °C) were obtained as the slope of the plots (Figure 5) by linearization of the test data in an integral form of rate equations, Φ , presented in [15].

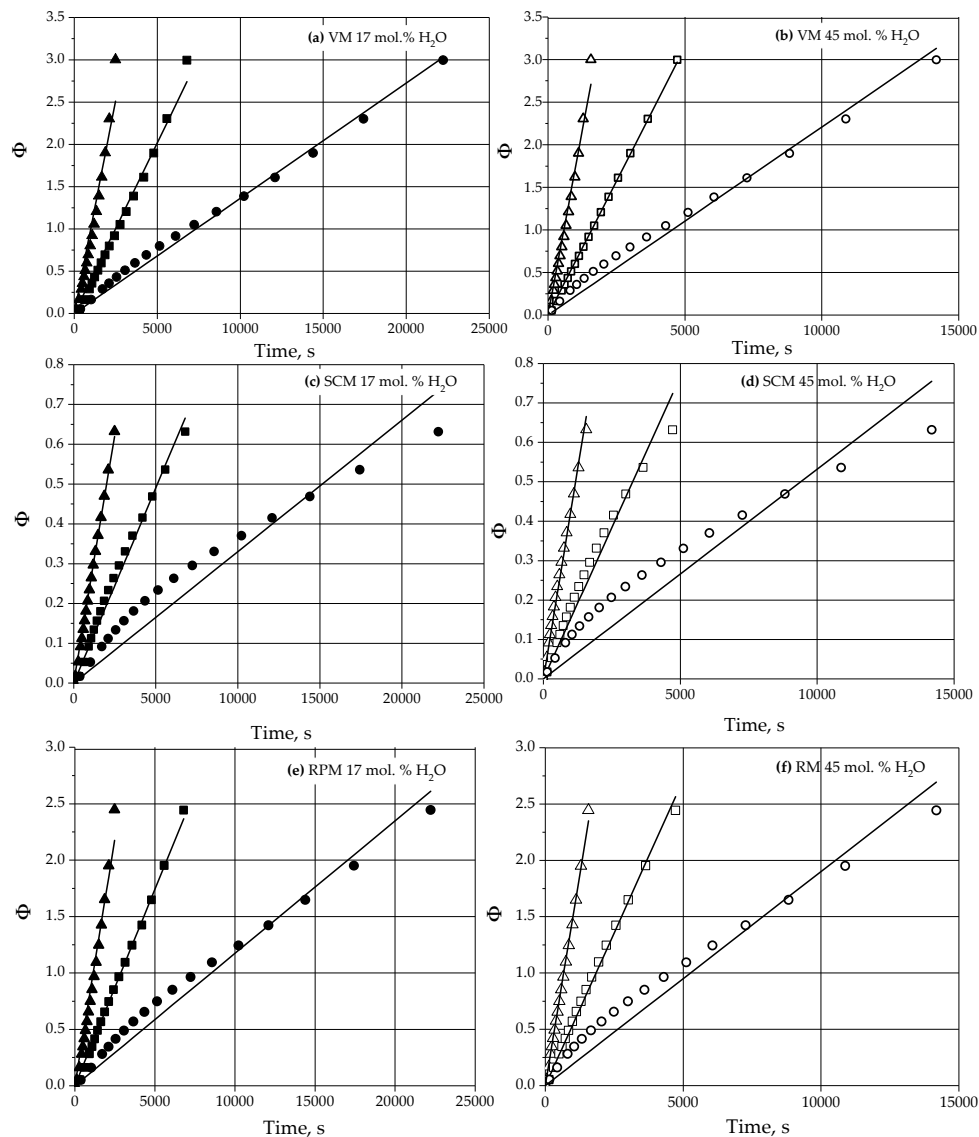


Figure 5. Linearization of the test data with three model equations (RPM, SCM, VM) for the gasification of RPC char under different temperatures (750, 800 and 850 °C) and steam mole fractions (0.17 and 0.45). The symbols show test data, and the solid lines are their linear fits as predicted by the linear regressions (symbol markings as in Figure 4).

If any model is valid, i.e., if the model adequately predicts the experimental data, then the plots of those data presented in Figure 5 should be a straight line. As seen from Figure 5, this condition seems to be better fulfilled by the VM and RPM than by the SCM, particularly at the lowest temperature.

The structural parameter ψ needed for the calculation of Φ in the RPM can be determined from the maximum of the experimental reaction rate profiles [34]. However, as shown in Figure 4, estimating the maximum position on the reaction rate curves may not be accurate or may be simply impossible. In this study, the structural parameter (ψ) was calculated by fitting Equation (4) to the experimental data (as shown in Figure 6 using nonlinear regression analysis as proposed by [35])

$$\frac{t_X}{t_{0.95}} = \frac{\sqrt{1 - \psi \ln(1 - X)} - 1}{\sqrt{1 - \psi \ln(1 - 0.95)} - 1} \quad (4)$$

where $t_{0.95}$ is the time for 0.95 carbon conversion, t_X is the time after which the conversion is X . The structural parameter, $\psi = 0.37$, was determined.

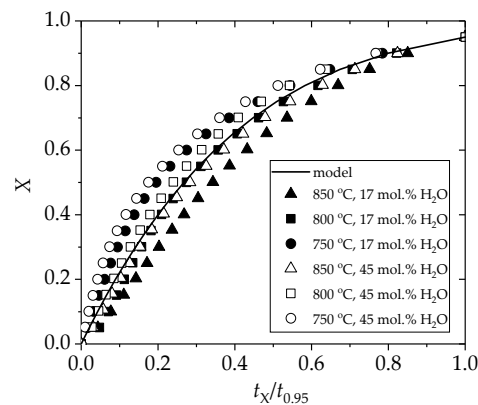


Figure 6. Comparison of the conversions obtained from Equation (4), and measured in this work for the structural parameter.

Then, the initial values of activation energy (E), the reaction order (n), the pre-exponential factor (A) of the RPC char- H_2O reaction at different steam concentrations and temperatures for each of the kinetic models were determined from the Arrhenius and $\ln k_s$ vs. y_g plots. Figure 7 shows examples of plots for the VM.

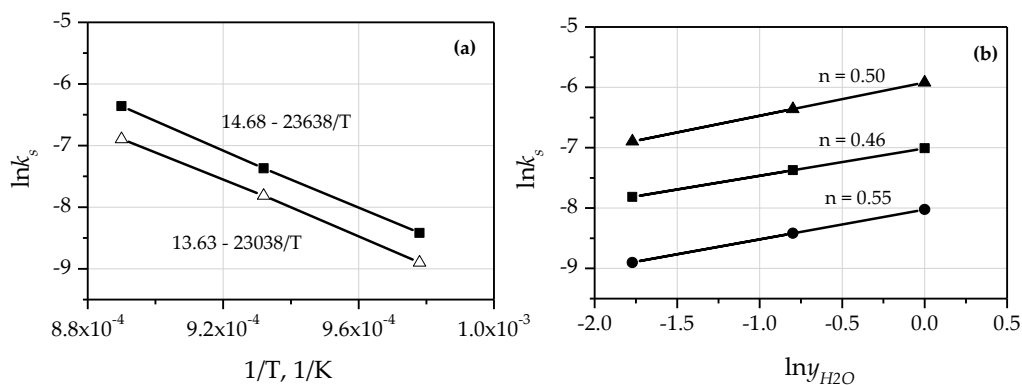


Figure 7. (a) Determination of the Arrhenius parameters and (b) the reaction order with respect to the molar fraction of steam for the volumetric model (VM) rate equation. Symbol markings as in Figure 6.

In second step of our kinetic study, the final model parameters were estimated with use of three rate equations with a nonlinear regression of the test data. In order to obtain the Arrhenius parameters and the reaction order with respect to steam mole fractions (0.17 and 0.45), the following expression (Equation (5)) was used

$$SSR(A, E, n, \psi) = \sum_{i=1}^M \sum_{j=1}^N \left(X_{i,j}^{\text{exp.}} - X_{i,j}^{\text{cal.}} \right)^2 \quad (5)$$

where n ($n = 20$, in this analysis) is the number of test data points in each run, M ($M = 6$ in this analysis) is the number of test runs, $X^{\text{cal.}}$ and $X^{\text{exp.}}$ is the RPC char conversion predicted and specified experimentally from the rate equation of steam gasification presented in [15]. In the calculations, the parameter was not taken as a fitting parameter in the RPM and a previously determined value, $\psi = 0.37$, was used.

The optimum values of the kinetics parameters and minimum SSR values in three models (VM, SCM, RPM) are given in Table 3. It can be seen that the VM yields the lowest residual sum of squares between the observed and predicted values of conversion so it seems to be the most suitable model for predicting the behavior of the RPC char gasification with steam at temperatures of 750–850 °C and steam concentrations less than 0.45 mole fraction. It is worth emphasizing that the RPM can well predict the CO_2 gasification of the RPC char as was reported in our previous study [15].

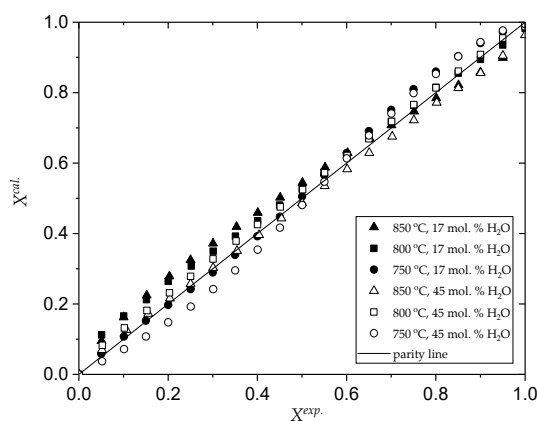
Table 3. Optimal values of the kinetic parameters of RPC char samples for different models.

Model	A, s^{-1}	$E, kJ \cdot mol^{-1}$	$n, -$	$\psi, -$	SSR, -
VM	$1.18 \cdot 10^5$	166.0	0.50	-	0.133
SCM	$3.93 \cdot 10^5$	187.7	0.61	-	0.255
RPM	$2.39 \cdot 10^5$	172.3	0.54	0.37	0.186

A comparison of the conversion is presented in Figure 3, and it was calculated by using the rate equation (Equation (6)) derived for the pseudo-homogeneous volumetric model with the parameters given in Table 3 and the experimental data.

$$\frac{dX}{dt} = 1.18 \cdot 10^5 \exp\left(-\frac{166}{RT}\right)(1-X)y_{H_2O}^{0.5}, s^{-1} \quad (6)$$

The good fit of the VM is also confirmed by the parity plots shown in Figure 8, where the experimental data lie very close to the main diagonal, which represents the perfect fit.

**Figure 8.** Plots for the VM rate equation.

The kinetic equation determined in this work could be helpful in modeling and designing of a reactor for steam gasification of RPC char or for gasification of RPC in a conventional (one step) process where the reaction of char with a gasification agent is the rate limiting step in the overall process.

4. Conclusions

In summary, steam gasification of pyrolysis RPC char was studied in a thermo-balance coupled with mass spectrometer (TGA-MS) at atmospheric pressure to determine the composition of the gas products and the ability of three kinetic models (the volumetric model, the shrinking core model and the random pore model) to predict the conversion of the char versus time. It has been found that steam gasification of the RPC-derived char produces synthesis gas with a molar ratio of H_2/CO that is favorable for methanol synthesis. However, due to the high CO_2 content (approximately 28 mol %), the synthesis gas should be subjected to additional treatment before entering the synthesis reactor. Under realistic gasification conditions a different synthesis gas composition can be obtained using a mixture of steam and carbon dioxide and temperature.

Using the lowest residual sum of squares between the observed and predicted values of conversion as a selection criterion, the best-fitting model was the pseudo-homogeneous volumetric model. The activation energy and the reaction order with respect to steam are equal to 166 kJ/mol and 0.5, respectively, and are typical values for the gasification of biomass chars with steam.

Author Contributions: Conceptualization, L.N. and D.S.; formal analysis, L.N., D.S. and M.M.; investigation, M.M.; writing—original draft preparation, L.N. and D.S.; writing—review and editing, D.S. All authors have read and agreed to the published version of the manuscript.

Funding: This research received no external funding.

Conflicts of Interest: The authors declare no conflict of interest.

Nomenclature

A	pre-exponential factor, s^{-1}
Ar	argon
CH ₄	methane
CO	carbon monoxide
CO ₂	carbon dioxide
E	activation energy, $\text{kJ}\cdot\text{mole}^{-1}$
H/C	hydrogen to carbon ratio
H ₂	hydrogen
H ₂ S	hydrogene sulfure
k_s	first order reaction rate constant, s^{-1}
k	reaction rate constant independent of H ₂ O concentration, s^{-1}
KOH	potassium hydroxide
m_0	initial weights of the sample during the reaction, g
m	final mass of the sample at the end of gasification, g
m_F	actual mass of the sample during the reaction, g
MS	mass spectrometer
n	order of reaction,-
NaOH	rapeseed press cake
r_s	intrinsic reaction rate, s^{-1} or $\text{m}\cdot\text{s}^{-1}$
RPC	rapeseed press cake
RPM	random pore model
SCM	shrinking core model
SNG	synthetic natural gas
T	temperature, K
t	time, s
TGA	thermogravimetric analyser
X	conversion,-
y_g	concentration of H ₂ O in the gas stream, mol. fraction
WGS	water-gas shift reaction
VM	volumetric model
Greek	symbols
ψ	structural parameter

References

1. Fukuda, H.; Kondo, A.; Noda, H. Biodiesel fuel production by transesterification of oils. *J. Biosci. Bioeng.* **2001**, *92*, 405–416. [[CrossRef](#)]
2. Leung, D.Y.C.; Wu, X.; Leung, M.K.H. A review on biodiesel production using catalyzed transesterification. *Appl. Energy* **2010**, *87*, 1083–1095. [[CrossRef](#)]
3. Musa, I.A. The effects of alcohol to oil molar ratios and the type of alcohol on biodiesel production using transesterification process. *Egypt. J. Pet.* **2016**, *25*, 21–31. [[CrossRef](#)]
4. Willems, P.; Kuipers, N.J.M.; De Haan, A.B. Hydraulic pressing of oilseeds: Experimental determination and modeling of yield and pressing rates. *J. Food Eng.* **2008**, *89*, 8–16. [[CrossRef](#)]
5. Özçimen, D.; Karaosmanoğlu, F. Production and characterization of bio-oil and biochar from rapeseed cake. *Renew. Energy* **2004**, *29*, 779–787. [[CrossRef](#)]
6. Ucar, S.; Ozkan, A.R. Characterization of products from the pyrolysis of rapeseed oil cake. *Bioresour. Technol.* **2008**, *99*, 8771–8776. [[CrossRef](#)]
7. Smets, K.; Adriaensens, P.; Reggers, G.; Schreurs, S.; Carleer, R.; Yperman, J. Flash pyrolysis of rapeseed cake: Influence of temperature on the yield and the characteristics of the pyrolysis liquid. *J. Anal. Appl. Pyrolysis* **2011**, *90*, 118–125. [[CrossRef](#)]

8. David, E.; Kopac, J. Pyrolysis of rapeseed oil cake in a fixed bed reactor to produce bio-oil. *J. Anal. Appl. Pyrolysis* **2018**, *134*, 495–502. [[CrossRef](#)]
9. Zhang, L.; Xu, C.; Champagne, P. Overview of recent advances in thermo-chemical conversion of biomass. *Energy Convers. Manag.* **2010**, *51*, 969–982. [[CrossRef](#)]
10. Dhyan, V.; Bhaskar, T. A comprehensive review on the pyrolysis of lignocellulosic biomass. *Renew. Energy* **2018**, *129*, 695–716. [[CrossRef](#)]
11. Onay, O.; Kockar, O.M. Slow, fast and flash pyrolysis of rapeseed. *Renew. Energy* **2003**, *28*, 2417–2433. [[CrossRef](#)]
12. Al Arni, S. Comparison of slow and fast pyrolysis for converting biomass into fuel. *Renew. Energy* **2018**, *124*, 197–201. [[CrossRef](#)]
13. Şensöz, S.; Yorgun, S.; Angin, D.; Çulcuoğlu, E.; Özçimen, D.; Karaosmanoğlu, F. Fixed bed pyrolysis of the rapeseed cake. *Energy Sources* **2001**, *23*, 873–876.
14. David, E.; Kopač, J. Upgrading the characteristics of the bio-oil obtained from rapeseed oil cake pyrolysis through the catalytic treatment of its vapors. *J. Anal. Appl. Pyrolysis* **2019**, *141*, 104638. [[CrossRef](#)]
15. Nowicki, L.; Siuta, D.; Markowski, M. Carbon Dioxide Gasification Kinetics of Char from Rapeseed Oil Press Cake. *Energies* **2020**, *13*, 2318. [[CrossRef](#)]
16. Chaudhari, S.T.; Bej, S.K.; Bakhshi, N.N.; Dalai, A.K. Steam Gasification of Biomass-Derived Char for the Production of Carbon Monoxide-Rich Synthesis Gas. *Energy Fuels* **2001**, *15*, 736–742. [[CrossRef](#)]
17. Chaudhari, S.T.; Dalai, A.K.; Bakhshi, N.N. Production of Hydrogen and/or Syngas (H₂ + CO) via Steam Gasification of Biomass-Derived Chars. *Energy Fuels* **2003**, *17*, 1062–1067. [[CrossRef](#)]
18. Motta, I.L.; Miranda, N.T.; Maciel Filho, R.; Wolf Maciel, M.R. Biomass gasification in fluidized beds: A review of biomass moisture content and operating pressure effects. *Renew. Sustain. Energy Rev.* **2018**, *94*, 998–1023. [[CrossRef](#)]
19. Zhang, X.; Brown, R.C. Introduction to Thermochemical Processing of Biomass into Fuels, Chemicals, and Power. *Thermochem. Process. Biomass* **2019**, 1–16. [[CrossRef](#)]
20. van Steen, E.; Claeys, M. Fischer-Tropsch Catalysts for the Biomass-to-Liquid (BTL)-Process. *Chem. Eng. Technol.* **2008**, *31*, 655–666. [[CrossRef](#)]
21. Bozzano, G.; Manenti, F. Efficient methanol synthesis: Perspectives, technologies and optimization strategies. *Prog. Energy Combust. Sci.* **2016**, *56*, 71–105. [[CrossRef](#)]
22. Ruoppolo, G.; Miccio, F.; Brachi, P.; Picarelli, A.; Chirone, R. Fluidized bed gasification of biomass and biomass/coal pellets in oxygen and steam atmosphere. *Chem. Eng. Trans.* **2013**, *32*, 595–600.
23. Pala, L.P.R.; Wang, Q.; Kolb, G.; Hessel, V. Steam gasification of biomass with subsequent syngas adjustment using shift reaction for syngas production: An Aspen Plus model. *Renew. Energy* **2017**, *101*, 484–492. [[CrossRef](#)]
24. Dayton, D.C.; Turk, B.; Gupta, R. Syngas Cleanup, Conditioning, and Utilization. *Thermochem. Process. Biomass* **2019**, 125–174.
25. Rauch, R.; Hrbek, J.; Hofbauer, H. Biomass gasification for synthesis gas production and applications of the syngas. *WIREs Energy Environ.* **2014**, *3*, 343–362. [[CrossRef](#)]
26. Kung, H.H. Deactivation of methanol synthesis catalysts—A review. *Catal. Today* **1992**, *11*, 443–453. [[CrossRef](#)]
27. González, J.F.; Román, S.; Encinar, J.M.; Martínez, G. Pyrolysis of various biomass residues and char utilization for the production of activated carbons. *J. Anal. Appl. Pyrolysis* **2009**, *85*, 134–141. [[CrossRef](#)]
28. Nowicki, L.; Ledakowicz, S. Comprehensive characterization of thermal decomposition of sewage sludge by TG–MS. *J. Anal. Appl. Pyrolysis* **2014**, *110*, 220–228. [[CrossRef](#)]
29. Nowicki, L.; Markowski, M. Gasification of pyrolysis chars from sewage sludge. *Fuel* **2015**, *143*, 476–483. [[CrossRef](#)]
30. Yan, F.; Luo, S.; Hu, Z.; Xiao, B.; Cheng, G. Hydrogen-rich gas production by steam gasification of char from biomass fast pyrolysis in a fixed-bed reactor: Influence of temperature and steam on hydrogen yield and syngas composition. *Bioresour. Technol.* **2010**, *101*, 5633–5637. [[CrossRef](#)]
31. Morin, M.; Pécate, S.; Masi, E.; Hémati, M. Kinetic study and modelling of char combustion in TGA in isothermal conditions. *Fuel* **2017**, *203*, 522–536. [[CrossRef](#)]
32. Blasi, C. Di Combustion and gasification rates of lignocellulosic chars. *Prog. Energy Combust. Sci.* **2009**, *35*, 121–140. [[CrossRef](#)]

33. Nowicki, L.; Siuta, D.; Godala, M. Determination of the chemical reaction kinetics using isothermal reaction calorimetry supported by measurements of the gas production rate: A case study on the decomposition of formic acid in the heterogeneous Fenton reaction. *Thermochim. Acta* **2017**, *653*, 62–70. [[CrossRef](#)]
34. Liu, G.; Benyon, P.; Benfell, K.E.; Bryant, G.W.; Tate, A.G.; Boyd, R.K.; Harris, D.J.; Wall, T.F. The porous structure of bituminous coal chars and its influence on combustion and gasification under chemically controlled conditions. *Fuel* **2000**, *79*, 617–626. [[CrossRef](#)]
35. Everson, R.C.; Neomagus, H.W.J.P.; Kaitano, R.; Falcon, R.; du Cann, V.M. Properties of high ash coal-char particles derived from inertinite-rich coal: II. Gasification kinetics with carbon dioxide. *Fuel* **2008**, *87*, 3403–3408. [[CrossRef](#)]



© 2020 by the authors. Licensee MDPI, Basel, Switzerland. This article is an open access article distributed under the terms and conditions of the Creative Commons Attribution (CC BY) license (<http://creativecommons.org/licenses/by/4.0/>).